www.czasopisma.pan.pl PAN POLSKA AKADEMIA NAUK www.journals.pan.pl

BULLETIN OF THE POLISH ACADEMY OF SCIENCES
TECHNICAL SCIENCES
Vol. 55, No. 2, 2007

Surface effects of adsorbed organic species on electrical properties of Au nanowires

C.M. LILLEY[1]* and R. MEYER[2]

[1]Department of Mechanical and Industrial Engineering, University of Illinois at Chicago, 842 W. Taylor Street (MC 251), Chicago, IL 60607 USA
[2]Department of Chemical Engineering, University of Illinois at Chicago, 810 S. Clinton (MC 110), Chicago, IL 60607 USA

Abstract. Effects from adsorption of organic species on the surface of nanomaterials have been investigated. Exposure to organic contaminants during material processing, handling and environmental exposure is unavoidable during the manufacturing process of nanoscale materials. In addition, at the nanoscale, surface area to volume ratios increase and surface effects will have an increasing influence on the material properties. Experimentally measured electrical properties of gold nanowires and composition will be presented. The results indicated that C, C—O—C and C=O are adsorbed at the surface of the gold nanowires. These surface contaminants are believed to cause the increase in measured resistivity. A theoretical study was performed to investigate diffusion of these contaminants into the first surface layer, which may act as scattering mechanisms for current flow.

Key words: nanowires, surface effects, electrical properties, gold.

1. Introduction

The research presented in this article is centered on investigating surface effects on measured properties of gold nanowires. Although bulk gold is considered to be an inert material, gold nanoparticles have been shown over the last 20 years to be catalytically active for a number of useful reactions [1]. In the investigation of the origin of the activity of nanosized gold, rough gold surfaces and the presence of undercoordinated atoms have been shown to be key factors in the ability of gold to activate certain molecules such as oxygen [2,3]. In addition, gold nanowires are of particular interest to nanomanufacturing because at the nanoscale, gold has unique optoelectronic properties with applications ranging from plasmonics [4,5] to high density arrays of interconnect junctions [6].

Despite the noble nature of bulk gold, it should be noted that even the low energy surfaces of gold can interact with simple adsorbates such as CO provided the pressure is high enough [7–10]. For example Jugnet et al. observed significant surface roughening and a lifting of terrace anisotropy of Au(110) for CO pressures above 0.1 mbar [9,10] which remained even after removal of CO. Scanning Tunneling Microscope (STM) images, following evacuation of CO, confirmed that the surface reorganization was accompanied by surface deposits which were believed to be carbon. Gold has even been proposed as a material for a CO sensor [11].

In addition, trace contaminants such as calcium and silicon can act as catalytic sites leading to the activation of oxygen [12,13]. Even when such impurities are present in small quantities, their effect upon the chemistry may be significant as their concentration at the surface may be much higher than their bulk concentration. This may be surprising at first glance because among metals gold possesses a very low surface energy. However, in a reactive environment such impurities may be stabilized at the surface and thereby will contribute significantly to catalysis [14]. Iizuka and co-workers recently presented evidence that the reactivity of Au powder could be tied directly to the concentration of silver at the surface [15]. Although low Miller index gold single crystal surfaces do not dissociate simple hydrocarbons under UHV conditions, the response of the surfaces to an ambient atmosphere is often quite different (as discussed above with CO). In fact, hydrocarbons are easily grafted to gold surfaces using thiol linkages [16,17]. Therefore, the in environment of electronic devices where exposure to various solvents and to air (oxygen) is almost unavoidable, even 'inert' gold nanowires are likely to be covered with adsorbates (or their products of decomposition) over time. Of course, when organic solvents such as alcohols decompose on the nanowire surface (whether catalyzed by trace contaminants, undercoordinated gold atoms or simply by the gold facets themselves), the atoms comprising these organic molecules (i.e. Oxygen (O), Carbon (C) and Hydrogen (H)) may not remain on the surface but rather may diffuse into the bulk.

At the bulk or macro- scale, these organic molecules do not significantly alter the electrical properties of the material. However, at the nanoscale, surface area to volume ratios become increasingly large and the dominance of surface effects emerges. Thus, the adsorbed contaminant at the surface of nanowires will have an important role on material properties. In this investigation, we will

*e-mail: clilley@uic.edu

present research that indicates increased electrical resistance attributed to organic molecules on the surface of gold nanowires. The increase in measured resistance is believed to result from diffusion of C and O into the subsurface and the bulk. The barriers to diffusion have been calculated for both contaminants on the Au(111) surface as well as migration from the surface to the subsurface and bulk diffusion from one low energy interstitial site to the next.

2. Experimental procedure for gold nanowire characterization

2.1. Sample preparation. The experimental procedure can be found elsewhere in more detail [18]. However, the fabrication process will be briefly outlined as follows: 1) Photoresist was patterned with e-beam lithography to form the rectangular cross section templates for nanowires with 100–300 nm in widths and with a lengths of 10 µm. 2) Gold was deposited with e-beam evaporation. 3) The photoresist was lifted-off to leave behind the gold nanowires with contact pads. Various samples with five and eight parallel wires between the contact pads were fabricated. An example of a five wire sample is shown in Fig. 1(a). Each sample was also imaged with Scanning Electron Microscopy (SEM) to measure the wire lengths and widths of the nanowires, see Fig. 1(b). The thickness was measured with a contact profilometer as 204 nm. A second die was also prepared during the gold deposition to analyze the film composition with X-ray Photoelectron Spectroscopy (XPS).

2.2. Experimental measurements. Detailed measurements of the carbon, oxygen, and nitrogen were carried out with multiple scans with XPS with a scanning resolution of 0.1 eV to investigate the presence of contaminants. Scans at multiple depths were also measured by etching into the gold with an argon ion gun in fifteen minute steps, see Fig. 2. Each fifteen minute etch step removed a thicknesses of approximately 20 nm of Au. A N-1s peak, at 398.4 eV, was not found in our scans [19] at the surface or with subsequent depth profiling. The XPS results show that the carbon and oxygen contaminants are mostly present on the surface of the gold. From a detailed survey scan of carbon, the profile of the peak was found to be asymmetric. The main peak for C 1s was measured at 283.9 eV. Two small peaks at 287.0 eV and 285.3 eV were also present. This indicated that carbon is not a pure amorphous structure [20]. The shifted two peaks indicate that C=O and C—O—C (or other decomposition products) were adsorbed on the surface.

Current-voltage measurements were made from which the resistance of the nanowires was calculated. Fig. 3 illustrates the resistance-current curves for samples fabricated with (a) 5 wires and (b) 8 wires. As indicated, some of the measured resistance curves were larger in value. It was suspected that some of the wires had been broken prior to testing which resulted in fewer nanowires being stressed versus the number patterned. This suspicion was confirmed upon inspection with SEM analysis during measurement of dimensions. Also, it can be clearly seen that with increasing current, the resistance becomes nonlinear. It is well known that gold has a positive temperature coefficient of resistance [21] and thus Joule heating is likely the dominant reason for a nonlinear current-voltage curve with larger bias voltages.

3. Effects of adsorbed organic species on electrical resistance

3.1. Data analysis of resistance as a function of surface area. To investigate surface effects from adsorbed organic species, the resistance of the gold nanowires was plotted as a function of surface area to volume ratio, see Fig. 4. Only three surfaces were exposed to the environment and therefore the surface area is defined as [18,22]:

$$A = (2tl + wl) \tag{1}$$

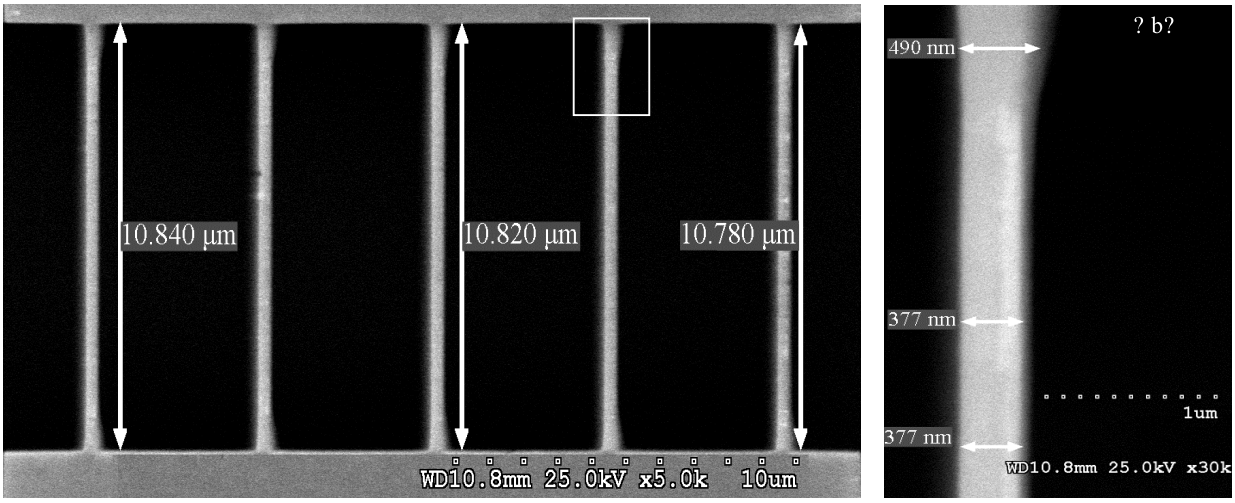

Fig. 1. SEM images of a five gold nanowires sample with (a) length measurements and (b) widths

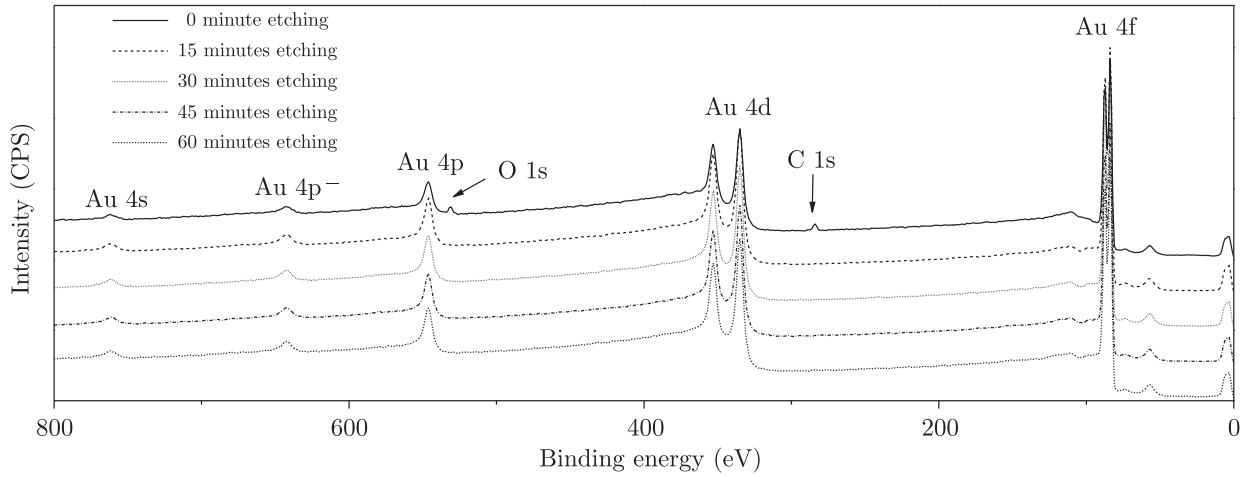

Fig. 2. XPS survey scans for depth profile: the surveys were scanned with etching steps of 15 minutes (from top to bottom curves). The curves have been vertically shifted for comparison of peaks

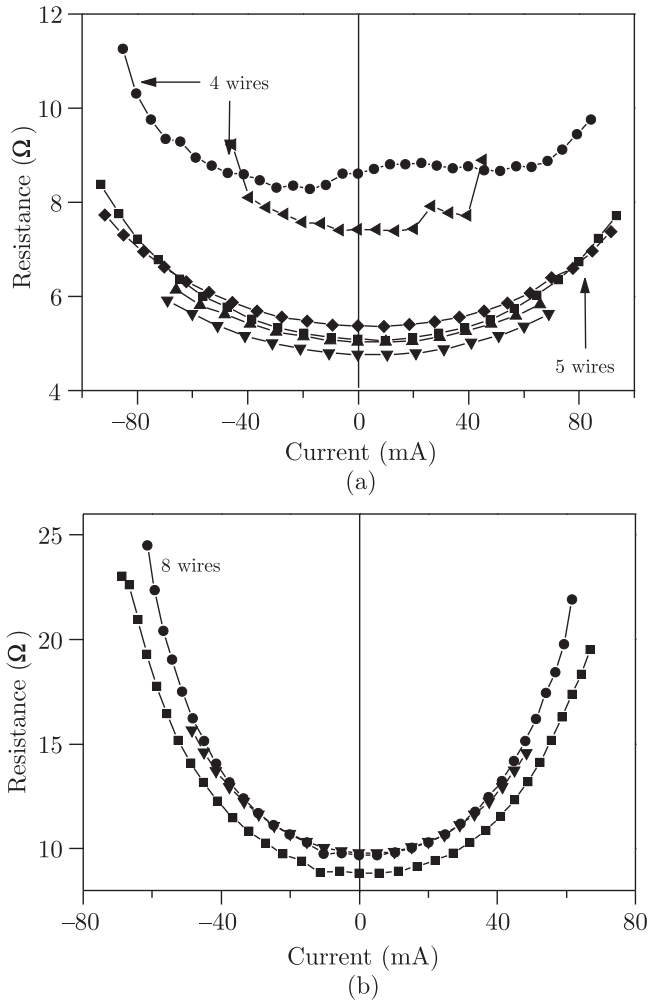

Fig. 3. Measured resistance curves for samples with (a) 5 wires ($l = 10$ μm, $w = 247$ nm and $t = 204$ nm; (b) 8 wires ($l = 10$ μm, $w = 117$ nm, and $t = 204$ nm)

where, t is the nanowire thickness, w is the width, and l is the wire length.

The ratio of the surface area to volume, x, can be expressed as:

$$x = A/(t \times w \times l) = 2/w + 1/t \tag{2}$$

The resistance R has a linear relationship with respect to x as follows:

$$R = ax + b \tag{3}$$

where,

$$a = \rho l/2t \tag{4}$$

and

$$b = \rho l/2t^2 \tag{5}$$

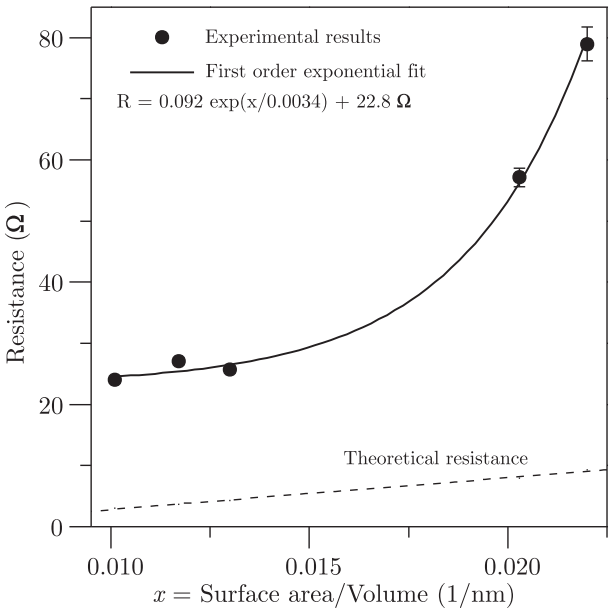

Fig. 4. Resistance normalized to a single wire plotted with respect to the surface area/volume. The straight line is the theoretical resistance when $\rho = 2.21 \times 10^{-8}$ Ω · m

Theoretical resistance values were calculated with a bulk resistivity of $\rho = 2.21 \times 10^{-8}$ Ω · m [21] for a single wire with a fixed length of 10 μm and a thickness

of 204 nm to compare with the measured trend of the gold nanowires. The tested gold nanowires had similar length to thickness dimensions as those plotted for the theoretical curve. However, it should be noted that since the resistance was measured with a two-point technique, therefore, the experimental data is shifted vertically because of the contact resistance for the probe. Direct comparison of the resistance was not made as a result; instead we looked at the shape of the measured curve. An exponential equation was fit to the experimental data, Eq. 3 $R = A \times exp(x/\tau) + B$. The calculated values were $A = 0.092\ \Omega$, $\tau = 0.0034\ \text{nm}^{-1}$, and $B = 22.8\ \Omega$. The measured constant B has a higher resistance value than that for the calculated bulk gold due to the contact resistance. However, we can see that as the nanowires become smaller, the resistance changes nonlinearly as compared to the theoretical resistance.

3.2. Analysis of experimental results. Previous research has shown nonlinear increases in resistance of gold nanowires from size effects that include wires with dimensions that approach the electron mean free path length and grain boundary scattering [23]. Durken and Wellend have published an extensive study of gold polycrystalline nanowires and modeled their results by combining the Fuchs Sondheimer (FS) and Mayada and Shatzkes (MS) theories; the combined theory takes into account surface scattering (FS) and grain boundary scattering (MS) respectively [23]. The wires tested had a thickness of 20 nm with various widths from 15 to 80 nm. The mean free path of 40 nm for polycrystalline gold at room temperature and a specular reflection coefficient of $p = 0.5$ was used to calculate the increased resistance from surface scattering. Their results show that for wires widths greater then 25 nm, there is no significant increase in resistance due to surface scattering. Also, increased resistance from grain boundary scattering is not significant for nanowires with widths larger than 60 nm. Therefore, the nonlinear increase in resistance for the results presented in the previous section should not be a result of surface or grain boundary scattering.

There are number of mechanisms for surface contamination to have an effect on the resistance of the gold nanowires. Some of these mechanisms include electron flow forced to tunnel through the wire instead of propagating on the surface resulting in increased grain boundary scattering and increased electron scattering at the surface from an insulating effect of an organic film. Since the organic films are only a few nanometers in thickness and are bonded to the surface with weak surface force attractions, it is unlikely that a surface only layer would be the dominant reason for the increased resistance. It is believed that the most likely mechanism is a result of diffusion of the organic contaminants into the subsurface and the bulk. The following sections discuss the diffusion paths for carbon and oxygen into the gold calculated with density functional theory. The calculations indicate that adsorption does occur at the surface of gold and that diffusion is likely, particularly for carbon, into the subsurface and bulk. Diffusion of these species into the gold would result in larger grain boundary scattering even with grains that are 100 nm or larger in size.

4. Computational methodology

Density functional theory calculations were performed using the program VASP (Vienna Ab initio Simulation Package), a DFT code for periodic systems [24,25]. The calculations utilized a plane wave basis set and ultrasoft pseudopotentials [26]. Exchange and correlation energies were calculated using the Perdew-Wang '91 form of the generalized gradient approximation [27]. Convergence tests were made with respect to the number of k-points and basis set size. A plane wave cutoff energy of 400 eV was used in all calculations. A $5 \times 5 \times 1$ k-point grid determined by the Monkhurst Pack method was employed for the 3×3 unit cell of the Au(111) surface [28]. Geometries were judged to be optimized when the forces were within a convergence tolerance of 0.01 eV/Å. Approximately four-layers of vacuum separated the five-layer Au slabs in the z-direction. Diffusion from the surface into the subsurface made use of the same 5 layer slab model. In this case the first three layers where allowed to relax during geometry optimizations (as opposed to only the first two layers in the surface diffusion calculations) while the bottom two layers where held fixed at their bulk values.

Diffusion of O and C atoms in the gold bulk were examined by using a 32 atom $2 \times 2 \times 2$ unit cell. Previously, Jiang and Carter examined C diffusion in austenite (fcc Fe) and found a 32 atom cell to be sufficiently large to characterize diffusion in the infinite dissolution limit [29]. A k-point sampling of $7 \times 7 \times 7$ was used for this unit cell. Various tests (described in the Results section) were performed to examine the distortion of the cell due to the presence of an impurity at an interstitial site.

Rate constants were calculated based on transition state theory using the climbing nudged elastic band method as described by Jonsson and coworkers [30]. This method involves the simultaneous optimization of a series of images that connect the reactant and product. In most cases the starting guess for the minimum energy path was derived from four images created by simple linear interpolation. A candidate for a transition state was identified as the maximum energy image along the optimized minimum energy path (movement is constrained to be perpendicular to the hyper-tangent). This potential transition state (if found) should have a force less than 0.05 eV/Åand it can be confirmed by a subsequent vibrational calculation revealing the presence of a single imaginary frequency. Vibrational calculations were performed by a diagonalization of the Hessian matrix created from the numerical second derivative of the energy with respect to each Cartesian coordinate.

5. Discussion of DFT results

As shown in Table 1, both oxygen and carbon are found to bind most strongly to the fcc threefold hollow sites of the Au(111) surface. A rough estimate to the diffusion barrier can be made by applying a simple hopping model to the diffusion process whereby the barrier is to be simply the difference between the lowest energy (most stable site) and the highest energy site over which the adsorbate must pass to move between low energy sites. In both cases, the bridge site is then assumed to be the transition state in the diffusion process. It should be mentioned that during the geometry optimization of carbon in the bridging site, the C atom always moved toward the more favorable hcp or fcc sites. Only by fixing the Au atoms in the surface layer in the xy-plane could the energy at the bridging site be estimated.

Table 1
Adsorption energy of carbon and oxygen on Au(111)

	atop	bridge	hcp	fcc
C	–2.06	–3.42	–4.01	–4.13
O	–1.52	–2.43	–2.61	–2.82

Notice: All energies in eV and a negative sign indicates an exothermic event

The barrier for C diffusion is found to be 0.71 eV, which is somewhat greater than the barrier for O diffusion of 0.39 eV. The barriers for surface diffusion are of interest of course because one can envision the decomposition of organic hydrocarbons on the gold surface far from grain boundaries or defects which might serve as conduits to subsurface diffusion. In this case, we expect rather rapid diffusion of both O and C across the Au(111) surface at room temperature given a standard pre-exponential factor of $1\times10^{13}s^{-1}$. It is interesting to note that the barriers for diffusion will scale with the adsorption energy at the most stable site. Mavrikakis et al. have found that the barrier for diffusion for simple adsorbates such as carbon and oxygen can be estimated as 12% of their binding energy or 0.34 eV and 0.50 eV respectively [31].

As mentioned above, grain boundaries, dislocations, defects and other features of an imperfect surface are expected to act as conduits to subsurface diffusion which might limit conductivity of Au nanowires under environmental exposure. However, before we examine this more complicated case, we wish to examine the barrier for diffusion from the ideal Au(111) surface into the subsurface. Two key sites in the subsurface are considered: octahedral and tetragonal interstitial sites. These sites are depicted in Fig. 5 (a) and (b) respectively and the results are listed Table 2. After relaxation, considerable rearrangement occurs. When C or O is inserted into the subsurface, the top layer of Au is pushed out as the O and C bonds lengthen from the ideal distances (as determined by the position of the interstitial tetragonal and octahedral sites in Au) and the surface exhibits significant buckling. For example the Au-O bond distance expands from 1.810 Å to 2.098 Å upon relaxation. The degree of interlayer expansion varied slightly from oxygen to carbon and from site to site, but in general the Au atoms tended to expand in the z-direction by 5–6%.

Table 2
Absorption energy of carbon and oxygen in Au(111) subsurface

	Octahedral	Tetragonal	Relaxed octahedral	Relaxed tetragonal
C	–2.86	–1.42	–3.77	–4.20
O	1.06	3.77	–1.33	–1.98

Notice: All energies in eV and a negative sign indicates an exothermic event

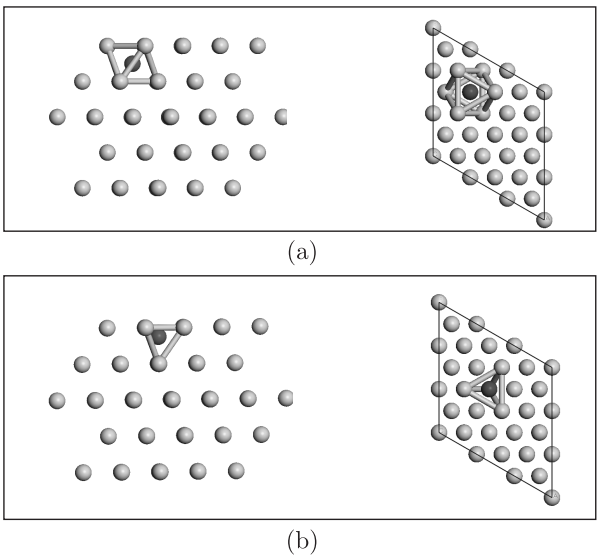

Fig. 5. Depiction of O absorption in Au(111) subsurface (a) Side and top view of octahedral site (b) side and top view of tetragonal site

Whereas C dissolution is exothermic even in the unrelaxed cell, the placement of O in the subsurface is highly unfavorable until surface relaxation can occur. Overall the adsorption of C and O in the subsurface is less favorable than adsorption on the Au(111) surface [32]. However, whereas small differences exist between the lowest energy surface site and the lowest energy subsurface site for C (in fact the placement of surface carbon into the subsurface is an exothermic event by 0.07 eV), these differences are substantial for oxygen. Before relaxation, both C and O prefer the octahedral position. After relaxation the tetragonal position is preferred. The barrier of diffusion from the surface to the subsurface has been determined from an examination of the path from the hcp site to the tetragonal site, see Table 5. In the case of oxygen, there is no additional barrier beyond the endothermic step of moving from the surface to the subsurface. Therefore, when the lowest energy site on the surface is considered (the fcc site as opposed to the hcp site) then the barrier of diffusion from the surface to the subsurface is estimated to be

0.84 eV. Our finding compares well with that of Fan et al. who found a barrier of 0.97 eV for the diffusion of oxygen from the surface to the subsurface of Ag(111) [33]. Incidentally since no additional barrier to diffusion exists and since the octahedral site is a higher energy site, then no possible lower energy pathway for surface to subsurface diffusion can exist. In contrast, for carbon a small barrier exists for diffusion to the subsurface which exceeds the energy of the subsurface site resulting in a barrier of 0.24 eV. This implies that the diffusion of surface carbon into the subsurface is actually controlled by the surface diffusion of carbon, as indicated by the potential energy surface diagram in Fig. 6. Although the barrier for oxygen diffusion indicates that diffusion into the subsurface would be slow at or near room temperature, Fan et al. have found that the presence of one adsorbate may affect the diffusion of a second. In their investigation, the presence of chlorine reduced the barrier to the diffusion of oxygen into the Ag(111) subsurface. Future work will explore such interactions between oxygen and carbon on Au. The surface coverages of carbon and oxygen were found to be somewhat higher in the XPS measurements than what we have chosen to model here. Furthermore, on the atomic scale, locale ensembles of carbon and oxygen may form which display different diffusion behavior. Therefore, future modeling efforts need to focus on not only the role of defect mediated diffusion, but also coverage effects on these processes.

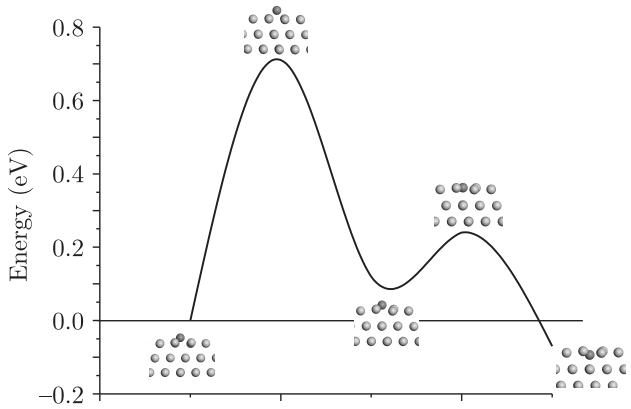

Fig. 6. Potential energy surface diagram showing diffusion of carbon from fcc site of Au(111) to the subsurface tetragonal site

Once the contaminant has reached the subsurface, it can diffuse in the bulk as well. We have used a slightly different model to evaluate bulk diffusion: a $2\times2\times2$ unit cell of fcc gold which corresponds to a system of 32 atoms for every heteroatom (or 3% concentration of the impurity by mole %). Once again the high symmetry octahedral and tetragonal interstitial sites have been considered as a starting point for describing the lowest energy sites available for both O and C. Results are given in Table 3. In the unrelaxed system, both C and O prefer to exist in the octahedral site as was the case for subsurface sites. Once again, the placement of O in interstitial sites was found to be endothermic whereas C absorbed exothermically.

Relaxation of the cell can be handled in multiple ways. First, we can simply allow the atoms to move while keeping the unit cell rigid. Secondly, we can allow the unit cell to expand while its shape is preserved. Lastly, we can allow not only the size but also the shape of the unit cell to change. The first case results in unrealistically high forces on the atoms, indicating a need to examine possibilities where the lattice can expand. As indicated in Table 4, the size of the unit cell is found to grow by almost 2% in the extreme case of O in the tetragonal site. This would seem to indicate that the energetics of O and C dissolution in gold are not quite converged with cell size, as one should see a lattice expansion of less than 1%. The third case is trivial, as the unit cell prefers to hold its cubic shape, therefore giving the same result as the second case.

Table 3
Absorption energy of carbon and oxygen in bulk Au

	Octahedral	Tetragonal	Relaxed octahedral	Relaxed tetragonal
C	–2.71	–0.75	–3.37	–3.44
O	1.16	4.03	–1.30	–1.63

Notice: All energies in eV and a negative sign indicates an exothermic event

Table 4
Lattice expansion

	Octahedral	Tetragonal
C	0.80	1.51
O	1.13	1.87

Notice: All expansions given as % and referenced to 32 atom unit cell

Table 5
Diffusion barriers of carbon and oxygen

	Surface	Surface to subsurface	Bulk
C	0.71	0.24	1.39
O	0.39	0.84	1.33

Notice: Units in eV After atomic relaxation in the expanded cell, we find that like the subsurface case, both O and C change their preferred adsorption site from the octahedral to the tetragonal site. A path between these lowest energy sites was constructed to determine a barrier for bulk diffusion. Surprisingly, as listed in Table 5, the barriers for bulk diffusion were found to be very similar: 1.33 and 1.39 eV for oxygen and carbon respectively. This can be rationalized by the similarity of their diffusion paths. It should be mentioned that attempts to find a low energy pathway between octahedral sites were unsuccessful. Further, it should be recognized that more complicated diffusion mechanisms are possible involving concerted movement of multiple atoms. This type of mechanism has been recently presented to explain the facile motion of vacancies in TiO_2 [32] as well as metal/metal diffusion processes.

6. Summary

As structural size decreases to the nanoscale, surface-area to volume ratio increases. With an increasing ratio, adsorption of organic species on the surface could affect the resistance of gold nanowires. Experiments were performed so that size effects were negligible and the results indicated a non-linear increase in resistance as a result of surface effects. XPS measurements indicated that C, C—O—C and C=O were adsorbed at the surface of the gold nanowires. As a result, diffusion of carbon and oxygen into Au(111) were investigated. The calculations indicate that diffusion of oxygen and, in particular, carbon along and into the surface is relatively facile even at temperatures near room temperature. Ultimately, it is suspected that these contaminants will collect at grain boundaries, thereby increasing grain boundary scattering. Further studies of defect mediated diffusion processes and grain boundary environments along with their effects on properties of nanowires are needed.

References

[1] G.C. Bond and D.T. Thompson, "Catalysis by gold", *Catal. Rev. Sci. Eng.* 41, 319 (1999).

[2] D.H. Wells, W.N. Delgass, and K.T. Thomson, "Density functional theory investigation of gold cluster geometry and gas-phase reactivity with O-2", *J. Chem. Phys.* 117, 10597 (2002).

[3] N. Lopez, T.V.W. Janssens, B.S. Clausen, Y. Xu, M. Mavrikakis, T. Bligaard, and J.K. Norskov, "On the origin of the catalytic activity of gold nanoparticles for low-temperature CO oxidation", *J. Catal.* 223, 232 (2004).

[4] A. Bouhelier, R. Bachelot, G. Lerondel, S. Kostcheev, P. Royer, and G.P. Wiederrecht, "Surface plasmon characteristics of tunable photoluminescence in single gold nanorods", *Phys. Rev. Lett.* 95, 267405 (2005).

[5] K.G. Thomas, S. Barazzouk, B.I. Ipe, Joseph, S.T.S. Joseph, and P.V. Kamat, "Uniaxial plasmon coupling through longitudinal self-assembly of gold nanorods", *J. Phys. Chem. B* 108, 13066–13068 (2004).

[6] N.I. Kovtyukhova, and T.E. Mallouk, "Nanowires as building blocks for self-assembling logic and memory circuits", *Chem. Eur. J.* 19, 4355–4363 (2002).

[7] F. Peters, P. Steadman, H. Isern, J. Alvarez, and S. Ferrer, "Elevated-pressure chemical reactivity of carbon monoxide over Au(111)", *Surf. Sci.* 467, 10 (2000).

[8] P. Steadman, K. Peters, H. Isern, J. Alvarez, and S. Ferrer, "Interaction of CO with the reconstructed Au(111) surface near atmospheric pressures", *Phys. Rev. B.* 62, R2295 (2000).

[9] Y. Jugnet, F.J.C.S. Aires, C. Deranlot, L. Piccolo, and J.C. Bertolini, "CO chemisorption on Au(110) investigated under elevated pressures by polarized reflection absorption infrared spectroscopy and scanning tunneling microscopy", *Surf. Sci.* 521, L639 (2002).

[10] L. Piccolo, D. Loffreda, F.J.C.S. Aires, C. Deranlot, Y. Jugnet, P. Sautet, and J.C. Bertolini, "The adsorption of CO on Au(111) at elevated pressures studied by STM, RAIRS and DFT calculations", *Surf. Sci.* 566, 995 (2004).

[11] C. Pupier, C. Pijolat, J.C. Marchand, and R. Lalauze, "Oxygen role in the electrochemical response of a gas sensor using ideally polarizable electrodes", *J. Electrochem. Soc.* 146, 2360–2364 (1999).

[12] M.E. Schraeder, "Chemisorption of oxygen to gold: AES study of catalytic effect of calcium", *Surf. Sci.* 78, L227 (1978).

[13] J.J. Pireaux, M. Chtaib, J.P. Delrue, P.A. Thiry, M. Liehr, and R. Caudano, "Electron spectroscopic characterization of oxygen-adsorption on gold surfaces substrate impurity effects on molecular-oxygen adsorption in ultra high-vacuum", *Surf. Sci.* 141, 211 (1984).

[14] B.C. Han, A. Van der Ven, G. Ceder, and B.J. Hwang, "Surface segregation and ordering of alloy surfaces in the presence of adsorbates", *Phys. Rev. B.* 72, 205409 (2005).

[15] Y. Iizuka, A. Kawamoto, K. Akita, M. Date, S. Tsubota, M. Okumura, and M. Haruta, "Effect of impurity and pretreatment conditions on the catalytic activity of Au powder for CO oxidation", *Catal. Lett.* 97, 203 (2004).

[16] T. Ishida, S. Tsuneda, N. Nishida, M. Hara, H. Sasabe, and W. Knoll, "Surface-conditioning effect of gold substrates on octadecanethiol self-assembled monolayer growth", *Langmuir* 13, 4638–4643 (1997).

[17] J.L. Trevor, K.R. Lykke, M.J. Pellin, and L. Hanley, "Two-laser mass spectrometry of thiolate, disulfide, and sulfide self-assembled monolayers", *Langmuir* 14, 1664–1673 (1998).

[18] C.M. Lilley and Q. Huang, "Surface contamination effects on resistance of gold nanowires", *Appl. Phys. Lett.* 89, 1 (2006).

[19] B.V. Crist, *Handbook of Monochromatic XPS Spectra*, *1. The Elements and Native Oxides*, Vol. 1, XPS International, 1999.

[20] J.F. Watts and J. Wolstenholme, *An Introduction to Surface Analysis by XPS and AES*, Wiley, 2003.

[21] D.R. Lide, *Handbook of Chemistry and Physics*, 75th ed., CRC, New York, 1996.

[22] C. Durkan and M.E. Welland, "Analysis of failure mechanisms in electrically stressed gold nanowires", *Ultramicroscopy* 82, 125–133 (2000).

[23] C. Durkan and M.E. Welland, "Size effects in the electrical resistivity of polycrystalline nanowires", *Phys. Rev. B* 61 (20), 14215–14218 (1999).

[24] G. Kresse and J. Furthmuller, "Efficient iterative schemes for ab initio total-energy calculations using a plane-wave basis set", *Phys. Rev. B* 54, 11169 (1996).

[25] G. Kresse and J. Furthmuller, "Efficiency of ab-initio total energy calculations for metals and semiconductors using a plane-wave basis set", *Comp. Mater. Sci.* 6, 15 (1996).

[26] D. Vanderbilt, "Soft self-consistent pseudopotentials in a generalized eigenvalue formalism", *Phys. Rev. B* 41, 7892 (1990).

[27] J.P. Perdew and Y. Wang, "Accurate and simple analytic representation of the electron-gas correlation-energy", *Phys. Rev. B* 45, 13244 (1992).

[28] H.J. Monkhurst and J.D. Pack, "Special points for Brillion-zone integrations", *Phys. Rev. B* 13, 5188 (1976).

[29] D.E. Jiang and E.A. Carter, "Carbon dissolution and diffusion in ferrite and austenite from first principles", *Phys. Rev. B* 67, (2003).

[30] G. Henkelman, B.P. Uberuaga, and H. Jonsson, "A climbing image nudged elastic band method for finding saddle

points and minimum energy paths", *J. Chem. Phys.* 113, 9901 (2000).

[31] A.U. Nilekar, J. Greeley, and M. Mavrikakis, "A simple rule of thumb for diffusion on transition-metal surfaces", *Angew Chem. Int. Edit.* 45, 7046 (2006).

[32] L.L. Jia, Y. Wang, and K.N. Fan, "Theoretical study of atomic oxygen adsorption on the chlorine-modified Ag(111) surface", *J. Phys. Chem. B* 107, 3813 (2003).

[33] H. Iddir, S. Ogut, P. Zapol, and N.D. Browning, "Diffusion mechanisms of native point defects in rutile TiO2", *Phys. Rev. B* 75, 073203 (2007).